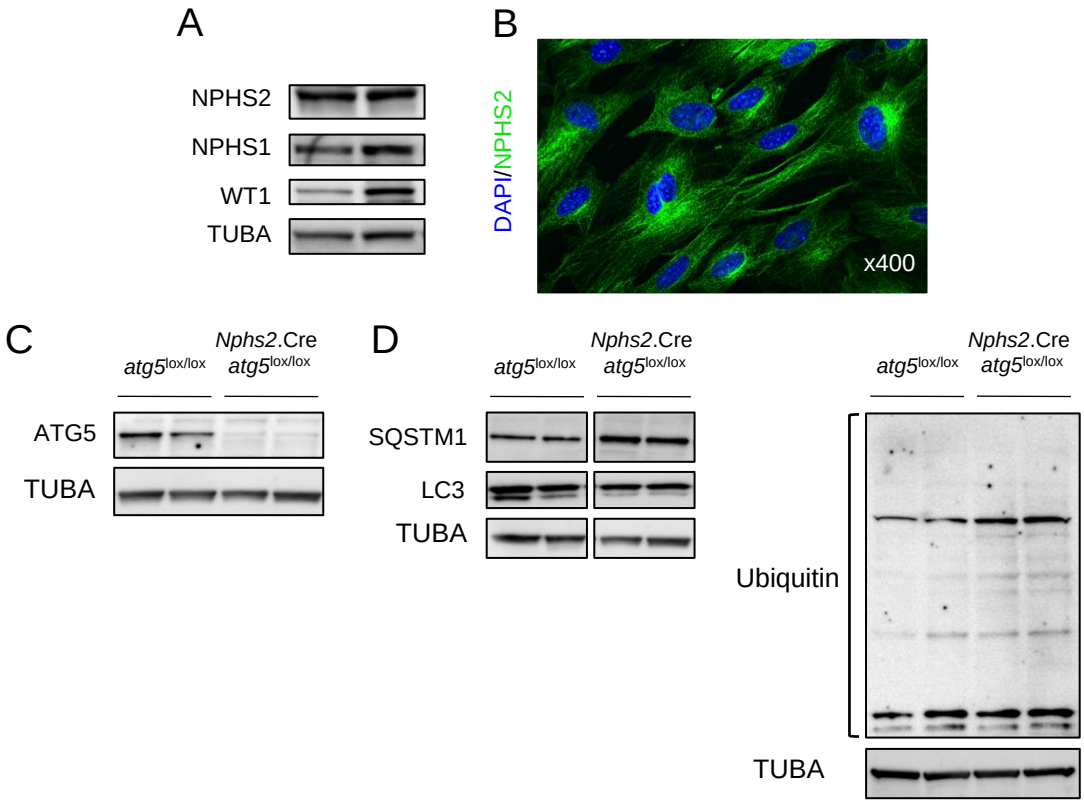

Supplementary Figure 1: Efficient deletion of Atg5 in podocytes from *Nphs2*.Cre *atg5*$^{lox/lox}$ mice. (A) Western blot analysis of the expression of NPHS2, NPHS1 and WT1 in primary podocytes culture from WT mice. Protein abundance is normalized to TUBA expression. (B) Representative images of the expression of NPHS2 (green) in primary podocytes culture. Nuclei are counterstained with DAPI (blue). (C) Western blot analysis of ATG5 expression in primary podocytes from WT and *Nphs2*.Cre-*atg5*$^{lox/lox}$ mice. Protein abundance is normalized to TUBA expression. (D) Western blot analysis of the expression of SQSTM1, LC3 and ubiquitinated proteins in primary podocytes from WT and *Nphs2*.Cre-*atg5*$^{lox/lox}$ mice. Protein abundance is normalized to TUBA expression.

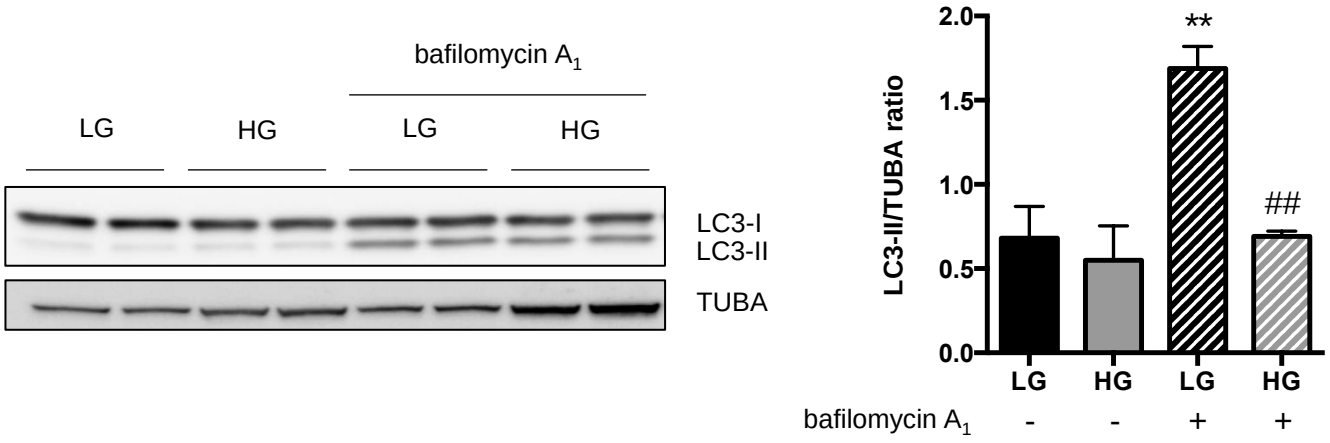

Supplementary Figure 2: Long-term treatment with high-glucose repress autophagic flux in podocytes. Western blot analysis of LC3 expression in SVI cells treated for 15 days with low-glucose (LG, 5 mM D-glucose) or high-glucose (HG, 33 mM D-Glucose), with or without bafilomycin A_1 (100 nM for 4 hours). Protein abundance is normalized to TUBA expression. Data represent means ± SEM of three independent experiments. ##, ** $p<0.01$. * different conditions of Bafilomycin A_1 treatment, same glucose concentration, # same conditions of bafilomycin A_1 treatment, different glucose concentration.

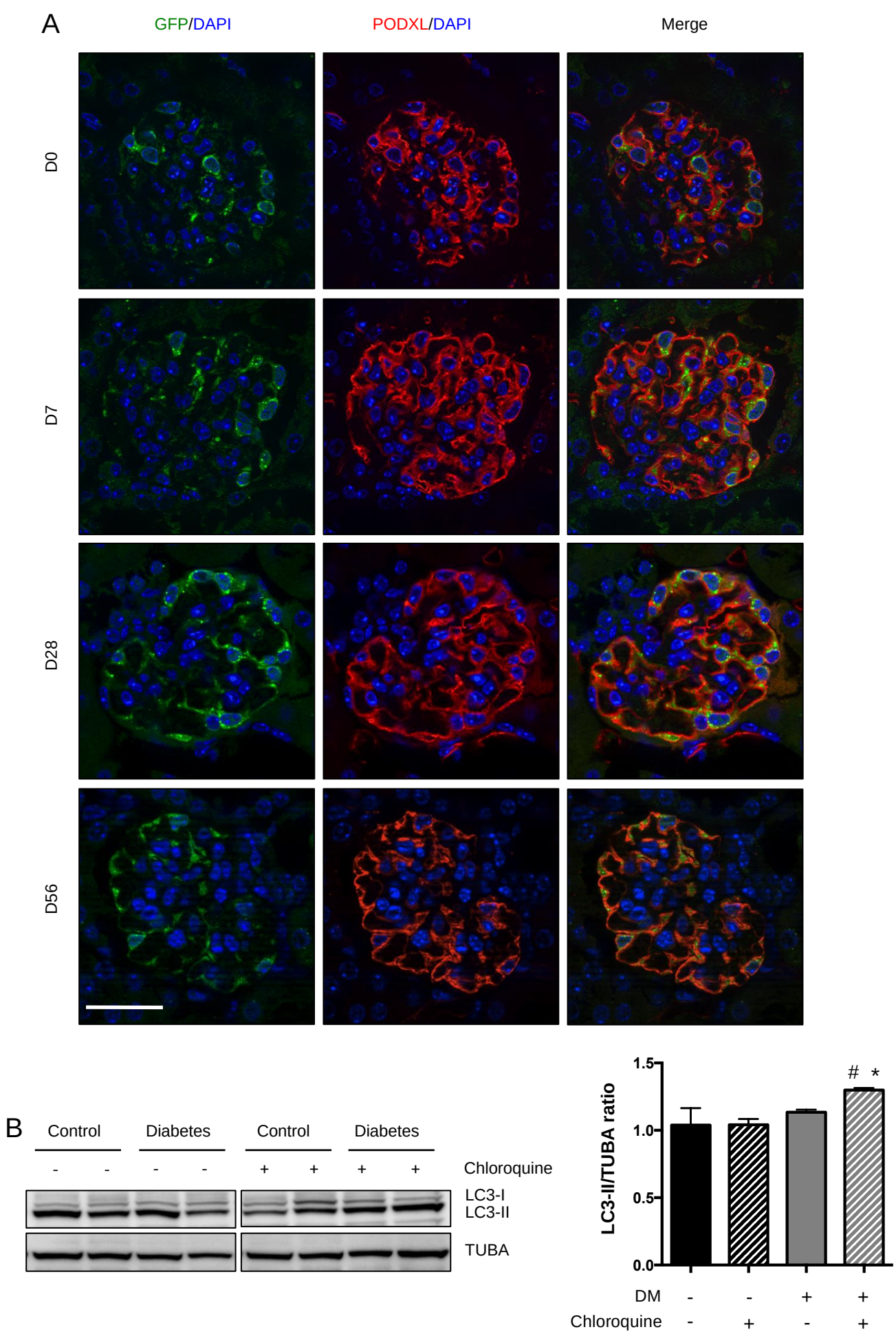

Supplementary Figure 3: Short-term hyperglycemia promotes autophagic flux in glomeruli, while long-term hyperglycemia represses autophagic flux. (A) Representative images of LC3 expression (green) in GFP-LC3 mice before STZ injection and 7, 28 or 56 days after STZ injection. The expression of LC3 is highest in podocytes, stained with PODXL (red), 28 days after the induction of diabetes. Nuclei are counterstained with DAPI stain (blue). Scale bar 20 µm. (B) Western blot analysis of LC3 expression in isolated glomeruli before STZ injection and 28 days after STZ injection, treated or not with chloroquine (50 mg/kg for 4 days before the sacrifice). Data represent means ± SEM of three mice. #, * $p<0.05$. * DM versus DM + chloroquine, # control + chloroquine versus DM + chloroquine.

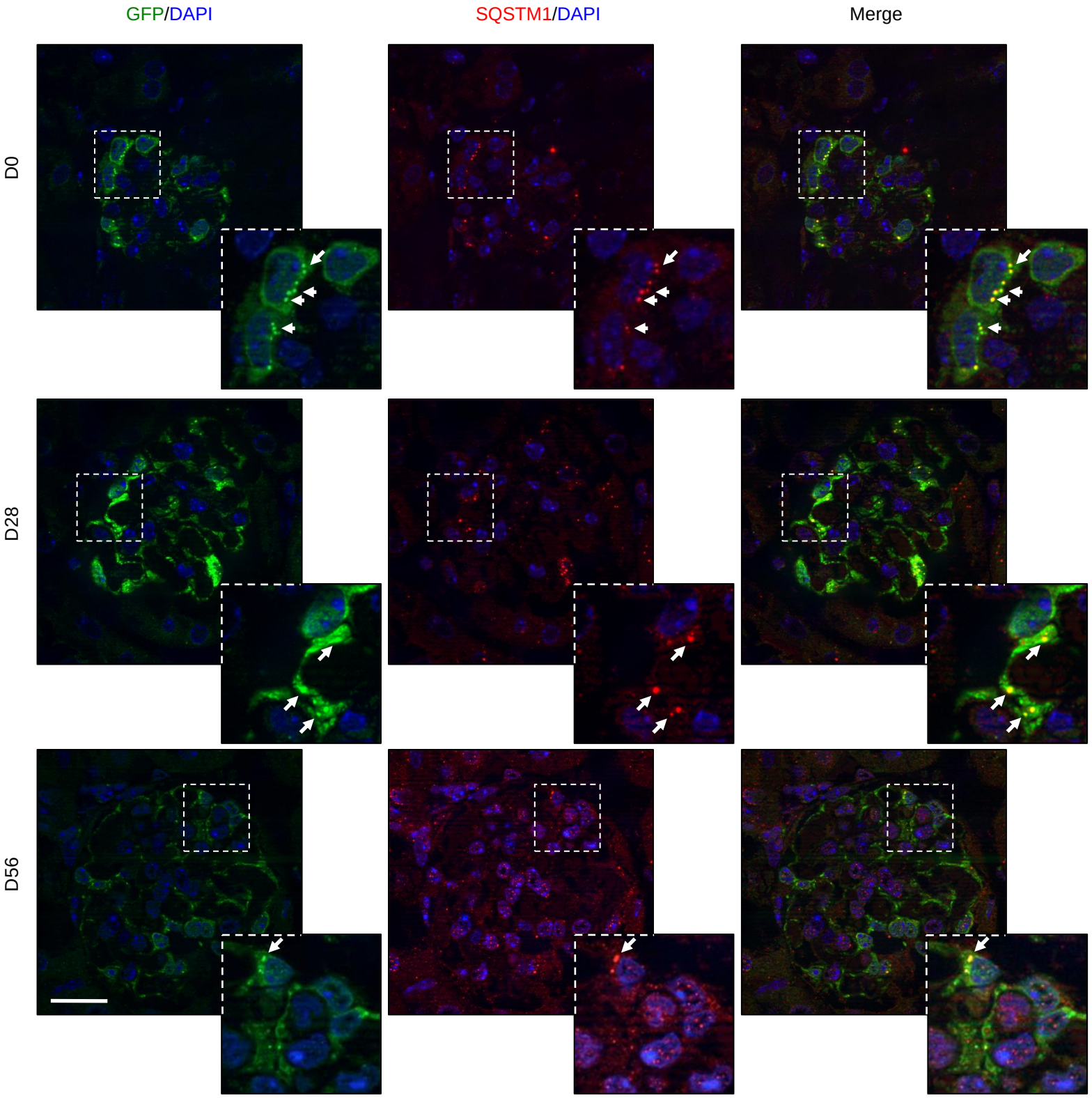

Supplementary Figure 4: Short-term diabetes promotes autophagic flux in glomeruli. Representative images of LC3 expression (green) and SQSTM1 (red) in GFP-LC3 mice before STZ injection and 28 or 56 days after STZ injection. Nuclei are counterstained with DAPI stain (blue). Scale bar 20 μm. Higher magnification are shown in the insets. Arrows show co-localization between LC3 and SQSTM1 in autophagosomes.

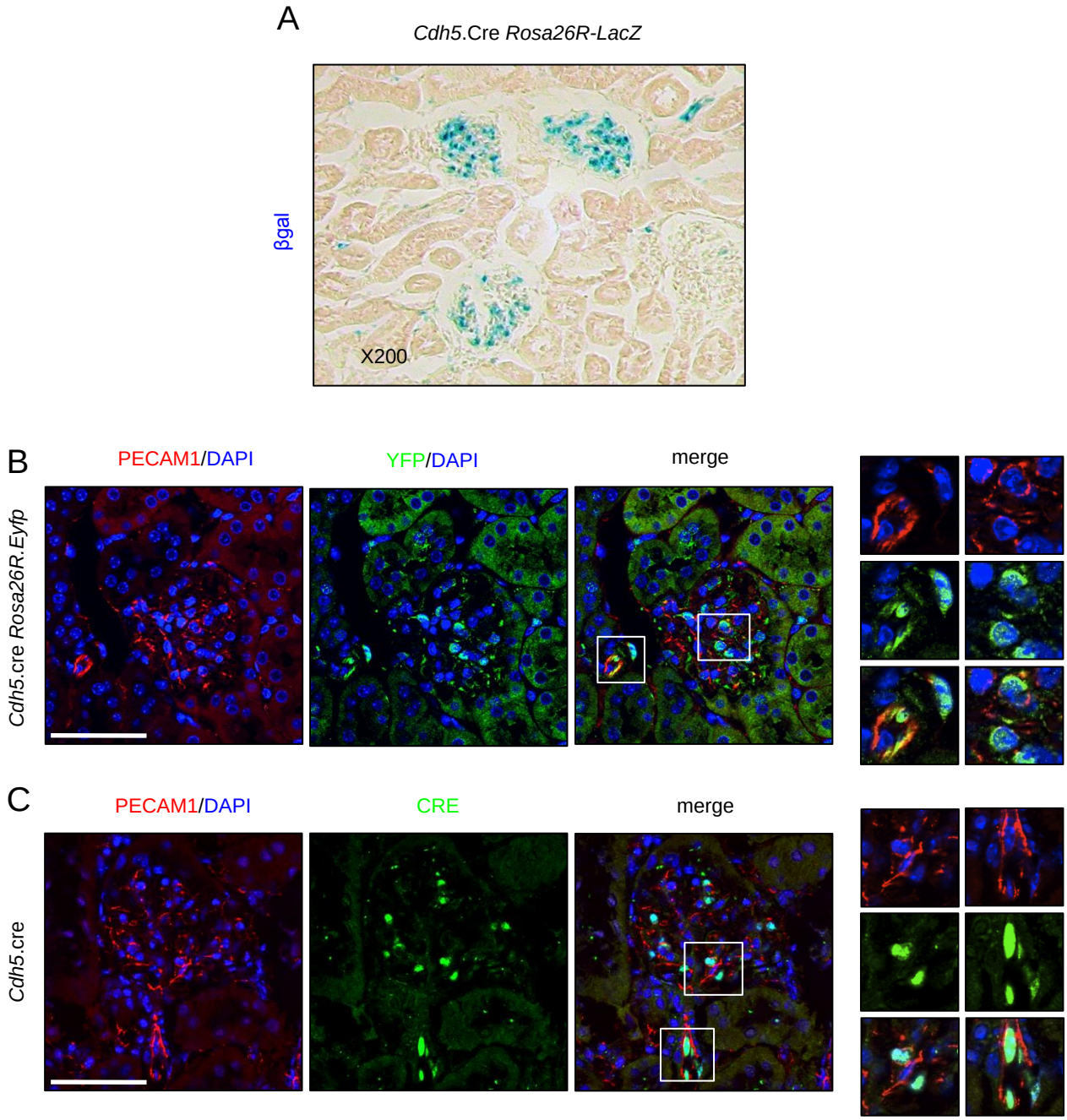

Supplementary Figure 5: Efficient CRE recombination in GECs in *Cdh5*.cre mice. (A) β-galactosidase staining in the cortex of *Cdh5*.cre *Rosa26R.LacZ* mice. (B) Representative images of YFP (green) in glomeruli of *Cdh5*.cre *Rosa26R.Eyfp* mice showing co-staining with the endothelial marker PECAM1 (red). (C) Representative images of CRE expression (green) in glomeruli of *Cdh5*.cre mice showing expression in endothelial PECAM1-positive cells (red). Nuclei are counterstained by DAPI stain (blue). Scale bar 50 μm.

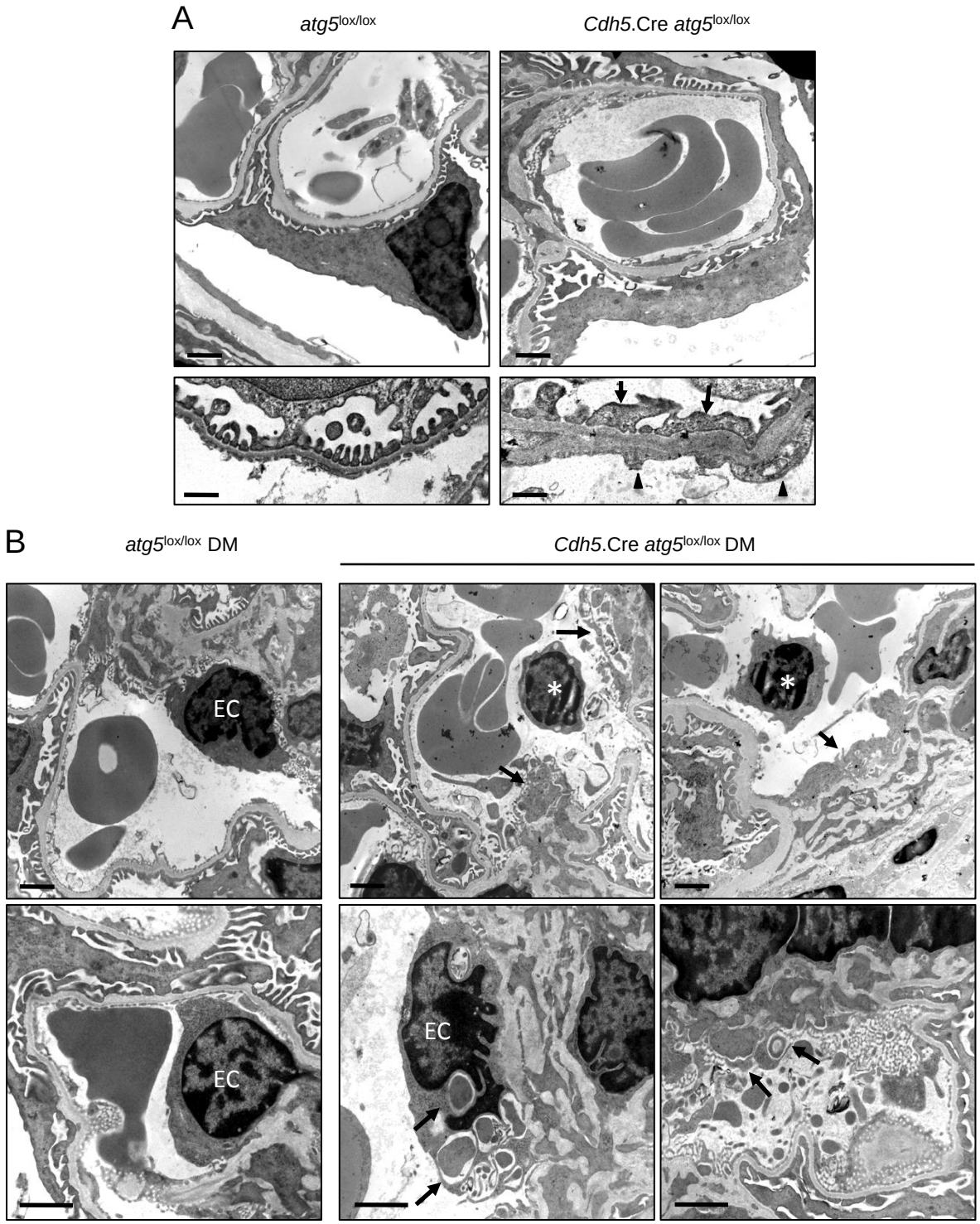

Supplementary Figure 6: Endothelial-selective deletion of *Atg5* specifically favors the development of glomerular endothelial lesions during diabetes. (A) Representative photomicrographs of transmission electron microscopy sections of glomeruli from 10 week-old WT and *Cdh5*.Cre-*atg5*$^{lox/lox}$ mice showing disappearance of endothelial fenestration (arrowheads) and podocyte foot process effacements (arrows) in *Cdh5*.Cre-*atg5*$^{lox/lox}$ mice. Scale bar 1 μm (upper panel) and 200 nm (lower panel). (B) Representative photomicrographs of transmission electron microscopy sections of glomeruli from 20 week-old WT diabetic and *Cdh5*.Cre-*atg5*$^{lox/lox}$ diabetic mice showing cells, most probably detached endothelial cells (EC), in the lumen of the capillaries (*) and cytoplasmic vacuolization (arrows) in *Cdh5*.Cre-*atg5*$^{lox/lox}$ diabetic mice. Scale bar 1 μm.

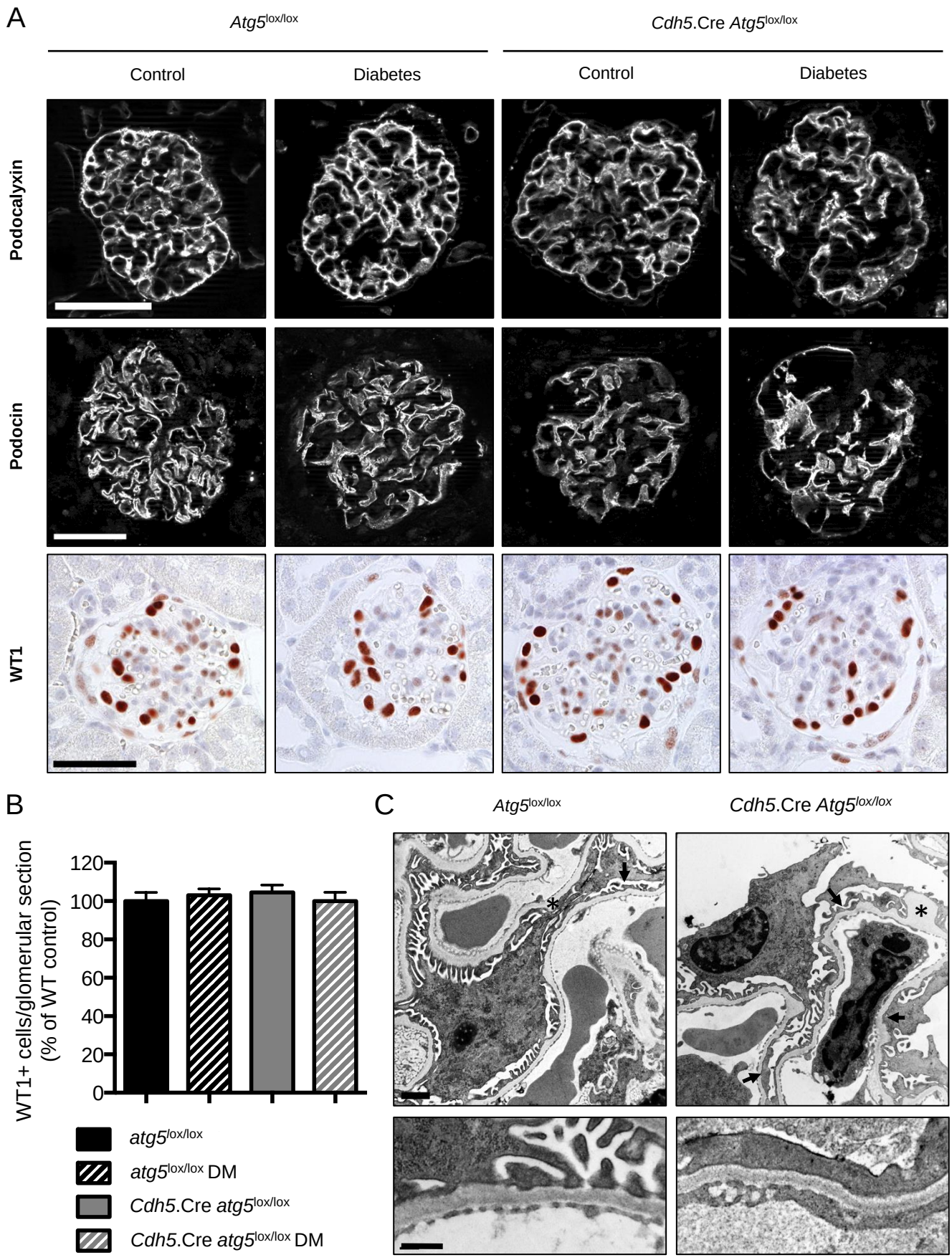

Supplementary Figure 7: **Autophagy deficiency specifically in endothelial cells promotes podocyte injury but not loss during diabetes.** (A) Representative images of the expression of PODXL (upper panel) and NPHS2 (middle panel) by immunofluorescence in 20 weeks-old WT control, WT diabetic, *Cdh5*.Cre-*atg5*$^{lox/lox}$ control and *Cdh5*.Cre-*atg5*$^{lox/lox}$ diabetic mice. Representative images of the expression of WT1 (lower panel) by immunohistochemistry in 20 weeks-old WT control, WT diabetic, *Cdh5*.Cre-*atg5*$^{lox/lox}$ control and *Cdh5*.Cre-*atg5*$^{lox/lox}$ diabetic mice. Images are representative of at least 6 mice. Scale bar 50µm. (B) Quantification of the glomerular WT1-positive cell numbers in 20 weeks-old WT control, WT diabetic, *Cdh5*.Cre-*atg5*$^{lox/lox}$ control and *Cdh5*.Cre-*atg5*$^{lox/lox}$ diabetic mice. Data are normalized to WT control and represent means ± sem of three mice. (C) Representative photomicrographs of transmission electron microscopy sections of podocytes from 20 weeks-old WT control, WT diabetic, *Cdh5*.Cre-*atg5*$^{lox/lox}$ control and *Cdh5*.Cre-*atg5*$^{lox/lox}$ diabetic mice showing GBM thickening (*) and foot process effacement (arrows) in WT and *Cdh5*.Cre-*atg5*$^{lox/lox}$ diabetic mice. Scale bar 1 µm (upper panel) and 200 nm (lower panel)